Closed-Form Phase and CFO Estimation CRLBs from Turbo-Coded PAM- and RQAM-Modulated Signals

Achref Methenni and Sofiène Affes
INRS-EMT, 800, De La Gauchetière West, Suite 6900, Montreal, QC, H5A 1K6, Canada.
Emails: {methenni, affes}@emt.inrs.ca

***Abstract*—We derive for the first time closed-form expressions for the Cramér-Rao lower bounds (CRLBs) of the joint channel phase, and carrier frequency offset (CFO) estimates from turbo-coded (TC) Pulse-amplitude modulation (PAM) and rectangular-QAM (RQAM) modulated signals over flat-fading channels. After wisely exploiting the properties of Gray mapping, we are able to simplify the log-likelihood function (LLF) to enable the CRLBs derivation in closed form. We show that the phase and the CFO can be *decoupled* if the set of sampling indices is centered on zero. These new bounds generalize those previously derived in closed form in the special case of TC square-QAM constellations or established empirically in the case of phase and CFO code-aided (CA) estimation, respectively. Numerical results suggest that the new CRLBs range between their respective CRLBs in the non-data-aided (NDA) and data-aided (DA) scenarios, thereby showcasing the expected advantage of CA estimation against both NDA and DA in terms of accuracy improvement or overhead reduction, respectively. They also illustrate the potential increase in estimation accuracy achievable by decreasing, as expected, the coding rate.**

***Index terms*—** Channel phase, Carrier frequency offset (CFO), Cramér-Rao lower bound (CRLB), Joint parameter estimation, decoupling, Turbo codes, Turbo processing, Gray labeling, extrinsic information, Code-assisted (CA), PAM, Rectangular QAM.

I. INTRODUCTION

Advanced wireless communication systems are intended to satisfy the ever increasing demand in high data rates while securing a good quality of service (QoS). One way to meet these requirements is to employ error correcting codes. In this regard, turbo codes have stirred a lot of interest in the last two decades [1] for their ability to achieve data rates near the Shannon limit for the wireless channel capacity, with a reasonable decoding complexity, thanks to the turbo principle. Another way to increase the throughput of the system is the use of high-order modulations, a key feature of current and future communication standards such as LTE, LTE-A and LTE-B [2]. In this context, high-order PAM and general QAM constellations are of extreme relevance.

Besides, *synchronization* is an important task the receiver has to accomplish in order to enable the best performance possible of the data transmission. Particularly, the channel phase is significant because it has a substantial effect on the performance of the system, especially if we use turbo codes. In fact, the latter are known to be highly sensitive to synchronization errors. That is, even a small shift in the channel phase can lead to severe performance degradations. The second fundamental parameter is the CFO, which has a tremendous impact as well on turbo codes, and thus on the bit error rate (BER) of the system, affecting thereby the networks' QoS.

These two parameters are generally unavailable at either side of the communication channel. That is why an estimation process is needed to acquire (approximately) these parameters [3]. Depending on the receivers' knowledge of the transmitted symbols, there are mainly two categories of estimators. The first class is that of NDA estimators which do not assume any *a priori* knowledge of the data and, hence, consider the received symbols independent and equally likely. The major asset of this approach is that it ensures high throughput since it requires no additional overhead and operates solely on the desired data sequence to be transmitted. However, it exhibits poor performance in the low-to-average SNR regime[1]. The second class of DA estimators exploits the fact that the pilot symbol sequence to deal with is known both to transmitter and the receiver. Although this method enhances the estimation accuracy since the symbols are known, it has the inconvenience of reducing the throughput of the system.

To circumvent the drawbacks on both ends, and in light of the use of powerful error correcting codes like turbo codes, a CA approach has emerged as a solution that combines both benefits of NDA and DA by offering a better estimation performance quality (compared to NDA), yet without the least overhead penalty on the overall throughput (compared to DA). This technique takes advantage of the decoding process and exploits the information it provides about symbols' probabilities to construct more accurate estimates of the desired parameters. Furthermore, using the turbo principle, CA estimators can be designed in an iterative fashion leading to far better performance. This process is called *turbo processing*. For instance, using the *a posteriori* probabilities and the *extrinsic* information, the carrier the CFO are estimated jointly with turbo decoding in [4].

Consequently, these estimators are reversely influenced by the performance of the decoding process: at one decoding iteration, an erroneous decoding of the received sequence will lead to a less accurate estimate. This interdependence between estimation and decoding in the CA scenarios renders the problem of finding the ultimate performance limit of such schemes more challenging. One such limit that addresses the best achievable estimation performance is the well-known fundamental CRLB [5] that sets the minimum achievable variance for any unbiased estimator. The derivation of closed-form expressions for the CRLBs in typical wireless communications scenarios is a difficult task, and sometimes an impossible one, because of the complex structure of the likelihood function, particularly for high-order modulations. This is why these bounds are usually evaluated empirically in most cases.

It was only recently, though, that the closed-form expressions for the stochastic CRLBs for the carrier phase and CFO NDA estimation have been established for BPSK/QPSK transmissions in [6], for general square-QAM-modulated signals in [7], and for general PAM and RQAM signals in [8], but still in the traditional NDA scenario. In coded transmissions, however, the likelihood

Work supported by the Discovery Grants and the CREATE PERSWADE <www.create-perswade.ca> Programs of NSERC and a Discovery Accelerator Supplement Award from NSERC.

[1] At high SNR, the estimator acts like DA, as if it knew the symbols.

978-1-5090-1328-9/16/$31.00 ©2016 IEEE

function (LF) becomes even more complicated and developing CRLB bounds in closed form becomes obviously much more challenging. Thus, exhaustive Monte-Carlo simulations have been recently used by Noels *et al.* in [9, 10] to evaluate *empirically* the CRLBs for CA estimates of the carrier phase and CFO parameters from turbo-coded linearly-modulated signals. Only recently, the CRLBs for these parameters estimates from turbo-coded square-QAM constellations were ultimately established in closed form [12].

Incited by all of the above-mentioned facts, we derive for the very first time analytical expressions for the CRLBs of the channel phase, and CFO estimates from turbo-coded general PAM and RQAM signals. These new bounds include the NDA case (when the bits' log-likelihood ratios (LLRs) are zero, i.e., the constellation symbols are equally likely) and the DA case (when the bits' LLRs are very large). They also corroborate previous works that derived them empirically [9, 10]. These bounds also show the advantage of CA over NDA and DA in terms of performance accuracy and signalling overhead, respectively, and the potential estimation gains achievable by decreasing the coding rate.

The remainder of this paper is organized as follows: In section II, we introduce the system model. In section III, we develop new expressions for the binary reflected Gray coded (BRGC) symbols' *a priori* probabilities (APPs) in the cases of general PAM and RQAM constellations in terms of their conveyed bits' log-likelihood ratios (LLRs). In section IV, we derive the LLFs of both modulation types. In section V, we ultimately derive novel closed-form expressions for the considered CRLBs and constellations. In section VI, we assess these new bounds by simulations. Finally, we draw out some concluding remarks in section VII.

II. System Model

Consider a wireless communication system where a binary sequence is grouped into blocks of equal length N_b bits per block. These data bits pass through a turbo encoder which consists of two identical recursive and systematic convolutional codes (RSCs) with different generator polynomials $[g1,\ g2]$, concatenated in parallel via an interleaver of size N_b. The overall coding rate R_c is fixed by the puncturer[2]. Each block of N_c coded bits is fed to an outer interleaver, and then labelled onto a Gray-coded constellation. The obtained symbols sequence travels over the wireless flat-fading channel. At the receiver side, the following processes are performed, consecutively:

1) Down-convert the received noisy signal to baseband by applying a rotation at a constant angular speed of $2\pi F$ rad/s where F is the carrier frequency. Due to the Doppler effect, the frequency mismatch between the oscillators of the transmitter and the receiver, and *synchronization* errors, this process results in a residual CFO. We assume the latter, denoted as ν, to be very small compared to the signal bandwidth.
2) Feed the obtained baseband signal to the matched filter of the transmit pulse $p(t)$. This pulse is supposed to verify the first Nyquist criterion.
3) Sample the signal at instants nT.

Throughout this paper, we assume *perfect timing synchronization*. In the presence of phase and CFO distortions, the observed samples are modeled as follows:

$$y_k \ = \ S\, x_k e^{j(2\pi k\nu+\phi)}+w_k, \quad k=k_0, k_0+1, \cdots, k_0+K-1, \ (1)$$

where, at the sampling index k (k_0 refering to the instant of the first sample), x_k is the k^{th} coded symbol transmitted over the wireless channel and y_k is its corresponding received sample. The channel is assumed to be slowly time-varying over the entire observation window of length K, and therefore has constant but unknown gain, S, and phase offset ϕ. The parameter ν stands for the normalized CFO, as mentioned before. The coded sequence x_k is drawn from any M-ary PAM or M_1xM_2-RQAM Gray-labeled constellation. Without loss of generality, we further assume the total energy of the transmitted sequence x_k to be unitary, i.e., $\mathrm{E}\{|x_k|^2\} = 1$. The additional term w_k stems from the noise components modeled by a sequence of zero-mean complex circular Gaussian random variables with independent real and imaginary parts, each of variance σ^2 (i.e., total noise power is $N_0 = 2\sigma^2$).

The true SNR, ρ, is defined as:

$$\rho \ = \ \frac{\mathrm{E}\{S^2|x_k|^2\}}{2\sigma^2} \ = \ \frac{S^2}{2\sigma^2}. \quad (2)$$

We wish to estimate the unknown phase and frequency offsets ϕ and ν, respectively. For this purpose, these parameters are stacked into a single parameter vector $\boldsymbol{\delta} = [\phi \quad \nu]$. For mathematical convenience, we gather as well all the recorded data samples in a single vector:

$$\boldsymbol{y} = [y_{k_0}, y_{k_0+1}, \cdots, y_{k_0+K-1}]^T. \quad (3)$$

Now suppose that we are able to produce an unbiased estimate, $\hat{\boldsymbol{\delta}}$, of the parameter vector $\boldsymbol{\delta}$, from the received vector $\boldsymbol{y}$. Then, the CRLB is a practical lower bound [5] that verifies[3] the inequality $\mathrm{E}\left\{[\hat{\boldsymbol{\delta}}-\boldsymbol{\delta}][\hat{\boldsymbol{\delta}}-\boldsymbol{\delta})]^T\right\} \succeq \ \mathrm{CRLB}(\boldsymbol{\delta})$ and is given by:

$$\mathrm{CRLB}(\boldsymbol{\delta}) = \boldsymbol{I}^{-1}(\boldsymbol{\delta}), \quad (4)$$

where $\boldsymbol{I}(\boldsymbol{\delta})$ is the Fisher information matrix (FIM) whose entries are expressed by:

$$[\boldsymbol{I}(\boldsymbol{\delta})]_{i,l} = -\mathrm{E}\left\{\frac{\partial^2 L(\boldsymbol{y};\boldsymbol{\delta})}{\partial\delta_i\partial\delta_l}\right\} \qquad i,l=1,2,3,4. \quad (5)$$

In (5), $\{\delta_i\}_{i=1,2,3,4}$ are the elements of the unknown parameter vector $\boldsymbol{\delta}$ and $L(\boldsymbol{y};\boldsymbol{\delta}) \triangleq \ln\left(p[\boldsymbol{y};\boldsymbol{\delta}]\right)$ is the LLF $\left(p[\boldsymbol{y};\boldsymbol{\delta}]\right.$ is the pdf of $\boldsymbol{y}$ parameterized by $\left.\boldsymbol{\delta}\right)$. As seen from (5), the first challenging step in deriving the targeted bounds is to find an explicit expression for the LLF or equivalently the pdf $p[\boldsymbol{y};\boldsymbol{\alpha}]$. To that end, the APPs, $P[x_k = c_m]$, of the transmitted symbols involved in (1) must be found. In the next section, we will express them in terms of the LLRs of the conveyed bits.

III. Derivation of the Symbols' APPs

Throughout this paper, we assume that the constellation is Gray labeled. Each point of the alphabet, $\{c_m\}_{m=1}^M$, is mapped onto a unique sequence of $\log_2(M)$ bits denoted here as $\bar{b}_1^m\bar{b}_2^m\cdots\bar{b}_l^m\cdots\bar{b}_{\log_2(M)}^m$. For the sake of clarity, this mapping will be denoted as follows:

$$c_m \longleftrightarrow \bar{b}_1^m\bar{b}_2^m\cdots\bar{b}_l^m\cdots\bar{b}_{\log_2(M)}^m. \quad (6)$$

The same notation is used to refer to the k^{th} bit sequence, $b_1^k b_2^k\cdots b_l^k\cdots b_{\log_2(M)}^k$, that is conveyed during the transmission of the k^{th} symbol x_k, i.e., $x_k \longleftrightarrow b_1^k b_2^k\cdots b_l^k\cdots b_{\log_2(M)}^k$. Due to the large-size interleaver, it is reasonable to assume that the coded bits are statistically independent. This is a standard assumption in CA

[2]This rate can be adjusted by changing the turbo code's puncturing matrix.

[3]For square matrices $\boldsymbol{A}$ and $\boldsymbol{B}$, $\boldsymbol{A}\succeq\boldsymbol{B}$ means $\boldsymbol{A}-\boldsymbol{B}$ is positive semi-definite.

estimation practices (see [9-11 and references therein). Therefore, the *a priori* probability of each transmitted symbol, x_k, factorizes into the elementary probabilities of its conveyed bits:

$$P[x_k = c_m] = P\left[\bigcap_{l=1}^{\log_2(M)} b_l^k = \bar{b}_l^m\right] = \prod_{l=1}^{\log_2(M)} P\left[b_l^k = \bar{b}_l^m\right]. \quad (7)$$

We also define the LLR of the l^{th} coded bit, b_l^k, conveyed by the transmission of the symbol, x_k, as follows:

$$L_l(k) \triangleq \ln\left(\frac{P[b_l^k = 1]}{P[b_l^k = 0]}\right). \quad (8)$$

Using (8) and the fact that $P[b_l^k = 0] + P[b_l^k = 1] = 1$, it can be easily shown that:

$$P[b_l^k = 1] = \frac{e^{L_l(k)}}{1 + e^{L_l(k)}} \quad \text{and} \quad P[b_l^k = 0] = \frac{1}{1 + e^{L_l(k)}}. \quad (9)$$

For every c_m in $\mathcal{C}$, if $x_k = c_m$, then the two identities in (9) can be merged together to yield a generic expression for the elementary probabilities involved in (7) as follows:

$$P[b_l^k = \bar{b}_l^m] = \frac{1}{2\cosh\left(\frac{L_l(k)}{2}\right)} e^{(\bar{b}_l^m - 1)\frac{L_l(k)}{2}}, \quad (10)$$

in which $\bar{b}_l^m$ is either 0 or 1 depending on which of the symbols c_m is transmitted, at time instant k, and of course on the Gray mapping that is associated to the constellation in (6). Therefore, injecting (10) in (7) and recalling that $\log_2(M) = p$ for PAM constellations, the symbols' APPs develop into:

$$P[x_k = c_m] = \underbrace{\left(\prod_{l=1}^{p} \frac{1}{2\cosh\left(\frac{L_l(k)}{2}\right)}\right)}_{\beta_k} \prod_{l=1}^{p} e^{(\bar{b}_l^m - 1)\frac{L_l(k)}{2}}. \quad (11)$$

Next, we describe a simple recursive procedure that permits the construction of arbitrary Gray-coded PAM and RQAM constellations.

A. PAM constellations:

A general PAM constellation, when $M = 2^p$ for any $p \geq 1$, is defined by:

$$\mathcal{C} = \{\pm(2i-1)d_p\}, \quad i = 1, 2, ..., 2^{p-1}, \quad (12)$$

where $2d_p$ is the intersymbol distance. Since the PAM constellation energy is supposed to be normalized to one, from which the expression of d_p is obtained as follows:

$$d_p = \sqrt{\frac{2^{p-1}}{\sum_{m=1}^{2^{p-1}}(2m-1)^2}}. \quad (13)$$

We now provide an outline of how to construct the Gray labeling of PAM constellations. In fact, starting from any given 2^{p-1}-PAM Gray-labeled constellation, it is possible to build another 2^p-PAM Gray-labeled constellation as follows:

- *Step 1*: Build the right half-space of the considered 2^p-PAM constellation from all the points of the considered 2^{p-1}-PAM constellation.
- *Step 2*: Build the left half-space of the new 2^p-PAM constellation by symmetry with respect to the y-axis. Now recall that the points of the original 2^{p-1}-PAM constellation represent just $p-1$ bits. Therefore, each point of the new 2^p-PAM constellation that must represent p bits is still missing one bit.
- *Step 3*: Add the missing bit that appears in each half-space of a basic BPSK constellation to all the points that appear in the same half-space of the new constellation.

It is easy to verify that this recursive procedure leads to a Gray-labelled constellation.

Another important property that can be drawn from this construction due to the symmetry in "*Step 2*" is that each two symbols $\tilde{c}_m$ and $-\tilde{c}_m$ share the same $p-1$ most significant bits (MSBs), $\bar{b}_1^m \bar{b}_2^m \bar{b}_3^m ... \bar{b}_{p-2}^m \bar{b}_{p-1}^m$, for any given symbol $\tilde{c}_m$ from the right half-space of the 2^p-PAM constellation. Thus, if we consider these $p-1$ MSBs and define:

$$\mu_k(c_m) \triangleq \prod_{l=1}^{p-1} e^{(2\bar{b}_m^l - 1)\frac{L_l(k)}{2}}, \quad \forall c_m \in \mathcal{C}, \quad (14)$$

it follows that:

$$\mu_k(\tilde{c}_m) = \mu_k(-\tilde{c}_m), \quad \forall \tilde{c}_m \in \tilde{\mathcal{C}}. \quad (15)$$

Then, we have:

$$P[x_k = \pm\tilde{c}_m] = \beta_k \ \mu_k(\tilde{c}_m) \ e^{\pm\frac{L_p(k)}{2}} \quad (16)$$

B. RQAM constellations:

A RQAM constellation can be defined, when $M = 2^{p_1+p_2}$ for any $p_1, p_2 \geq 1$ and $i = 1, 2, ..., 2^{p_1-1}; n = i = 1, 2, ..., 2^{p_2-1}$, as:

$$\mathcal{C} = \{\pm(2i-1)d_{p_1+p_2} \pm j(2n-1)d_{p_1+p_2}\}, \quad (17)$$

where $2d_{p_1+p_2}$ is the intersymbol distance[4]. Once again, we suppose the RQAM constellation energy to be unitary, from which the expression of $d_{p_1+p_2}$ is obtained as follows:

$$\frac{1}{d_{p_1+p_2}^2} = \sum_{i=1}^{2^{p_1-1}} \frac{(2i-1)^2}{2^{p_1-1}} + \sum_{n=1}^{2^{p_2-1}} \frac{(2n-1)^2}{2^{p_2-1}}. \quad (18)$$

We can easily demonstrate that this intersymbol distance can be expressed as a function of the intersymbol distances of the constituant unitary PAM constellations (i.e., unitary 2^{p_1}- and 2^{p_2}-PAMs) as folllows:

$$d_{p_1+p_2}^2 = \frac{1}{\frac{1}{d_{p_1}^2} + \frac{1}{d_{p_2}^2}}. \quad (19)$$

The Gray labeling for a $2^{p_1+p_2}$-QAM constellation is then constructed as follows :

- *Step 1*: Along the x-axis, Gray-label the real part of c_m (which represents a non unitary 2^{p_1}-PAM this time) using the same process for PAM Gray-labeling. The first p_1 MSBs $\bar{b}_1^m \bar{b}_2^m \cdots \bar{b}_{p_1}^m$ are thereby fixed.
- *Step 2*: Along the y-axis, Gray-label the imaginary part of c_m (which represents a non unitary 2^{p_2}-PAM as well) using again the very same process for PAM Gray-labeling. The remaining p_2 bits $\bar{b}_{p_1+1}^m \bar{b}_{p_1+2}^m \cdots \bar{b}_{p_1+p_2}^m$ are thereby fixed.
- *Step 3*: Adjunct the two groups of bits created in *Steps* 1 and 2, one next to the other. This completes the construction of the $2^{p_1+p_2}$-QAM constellation starting from two Gray-coded 2^{p_1}- and 2^{p_2}-PAM constellations constructed using the Gray-labeling process for PAM modulations presented in the previous subsection.

[4]The intersymbol distance for RQAM is defined by two integers, one for each dimension.

It is straightforward to show that this construction yields, from its use of two Gray-labeled PAM constellations, a Gray-labeled RQAM constellation. Since the coded bits are assumed independent, the real and imaginary parts of a rectangular $2^{p_1+p_2}$-QAM constellation symbol are also independent:

$$\begin{aligned} P[x_k=\tilde{c}_m] &= P[(\Re\{x_k\},\Im\{x_k\})=(\Re\{\tilde{c}_m\},\Im\{\tilde{c}_m\})] \\ &= P[\Re\{x_k\}=\Re\{\tilde{c}_m\}]\times P[\Im\{x_k\}=\Im\{\tilde{c}_m\}]. \end{aligned} \tag{20}$$

Treating the real and imaginary parts of the symbol $\tilde{c}_m$ like two PAM constellations and defining as in (14):

$$\mu_k(\Re\{c_m\}) \triangleq \prod_{l=1}^{p_1-1} e^{(2\bar{b}_m^l-1)\frac{L_l(k)}{2}}, \quad \forall c_m\in\mathcal{C}, \tag{21}$$

$$\mu_k(\Im\{c_m\}) \triangleq \prod_{l=p_1+1}^{p_1+p_2-1} e^{(2\bar{b}_m^l-1)\frac{L_l(k)}{2}}, \quad \forall c_m\in\mathcal{C}, \tag{22}$$

we can deduce, like in the PAM case, that:

$$\mu_k(\Re\{\tilde{c}_m\}) = \mu_k(-\Re\{\tilde{c}_m\}), \quad \forall\tilde{c}_m\in\tilde{\mathcal{C}}, \tag{23}$$

$$\mu_k(\Im\{\tilde{c}_m\}) = \mu_k(-\Im\{\tilde{c}_m\}), \quad \forall\tilde{c}_m\in\tilde{\mathcal{C}}. \tag{24}$$

Then, we have:

$$P[\Re\{x_k\}=\pm\Re\{\tilde{c}_m\}] = \beta_{k,1}\ \mu_k(\Re\{\tilde{c}_m\})\ e^{\pm\frac{L_{p_1}(k)}{2}}, \tag{25}$$

$$P[\Im\{x_k\}=\pm\Im\{\tilde{c}_m\}] = \beta_{k,2}\ \mu_k(\Im\{\tilde{c}_m\})\ e^{\pm\frac{L_{p_1+p_2}(k)}{2}}. \tag{26}$$

The above equations form the complete set of APPs for each symbol x_k. Note here that all the manipulations we have carried out previously to obtain the expressions for the APPs are intrinsic to the Gray-coded constellation only and do not need any assumption about the specific encoder used at the transmitter. Therefore, the CA CRLBs derived in this paper are actually valid for any coded transmission in general. In the evaluation of the CA CRLBs, however, as will be seen later, one needs accurate estimates for the bits' LLRs. And such estimates are obtained in turbo-coded systems from the output of the SISO decoder that is necessarily specific to the chosen codec (coder-decoder) implementation.

IV. Factorization of $p\big[y_k;\boldsymbol{\delta}\big]$

Recall from (5) that an explicit expression for the global LLF, $L(\boldsymbol{y};\boldsymbol{\delta}) \triangleq \ln\big(p[\boldsymbol{y};\boldsymbol{\delta}]\big)$, must be found before being able to derive the analytical CRLBs. Actually, since the coded bits are assumed to be statistically independent (due to the large-size interleaver), the transmitted symbols (which are simply some *soft* representations for different blocks of these bits) are also independent, thereby leading to:

$$p[\boldsymbol{y};\boldsymbol{\delta}] = \prod_{k=k_0}^{k_0+K-1} p[y_k;\boldsymbol{\delta}]. \tag{27}$$

Consequently, the global LLF breaks down to the sum of the elementary LLFs (pertaining to each received sample), i.e., $L(\boldsymbol{y};\boldsymbol{\delta}) = \sum_{k=k_0}^{k_0+K-1}\ln\big(p[y_k;\boldsymbol{\delta}]\big)$. Then, it can be seen from (1) that the pdf of each received sample, y_k, parameterized by the unknown parameter vector, $\boldsymbol{\delta}$, is given by:

$$\begin{aligned} p\big[y_k;\boldsymbol{\delta}\big] &= \sum_{c_m\in\mathcal{C}} P\big[x_k=c_m\big]\ p\big[y_k;\boldsymbol{\delta}|x_k=c_m\big] \\ &= \frac{1}{2\pi\sigma^2}\sum_{c_m\in\mathcal{C}} P\big[x_k=c_m\big]\exp\left\{\frac{|y_k-S_{\phi,\nu}c_m|^2}{2\sigma^2}\right\}, \end{aligned} \tag{28}$$

in which we use the shorthand notation $S_{\phi,\nu}\triangleq Se^{j(2\pi k\nu+\phi)}$. Then, denoting the inphase (I) and quadrature (Q) components of the received sample, respectively, as $I_k\triangleq\Re\{y_k\}$ and $Q_k\triangleq\Im\{y_k\}$, it can be shown that the pdf in (28) can be rewritten as follows:

$$p[y_k;\boldsymbol{\delta}] = \frac{1}{2\pi\sigma^2}\exp\left\{-\frac{I_k^2+Q_k^2}{2\sigma^2}\right\} D_{\boldsymbol{\delta}}(k), \tag{29}$$

in which the term $D_{\boldsymbol{\delta}}(k)$ is defined as:

$$\begin{aligned} D_{\boldsymbol{\delta}}(k) \triangleq \sum_{c_m\in\mathcal{C}} P[x_k=c_m]\exp\left\{-\frac{S^2\,|c_m|^2}{2\sigma^2}\right\} \\ \times\exp\left\{\frac{\Re\left\{c_m y_k^* S_{\phi,\nu}\right\}}{\sigma^2}\right\}. \end{aligned} \tag{30}$$

A. LLF for PAM signals:

The term $D_\delta(k)$ defined in (30) needs to be further developed in order to derive the analytical expressions for the considered CRLBs. When $M=2^p$ for any $p\geq 1$ (i.e., general PAM constellations), we have $\mathcal{C}=\{\pm(2i-1)d_p\}_{i=1,2,\ldots,2^{p-1}}$, where $2d_p$ is the intersymbol distance. Now by denoting $\tilde{\mathcal{C}}=\{+(2i-1)d_p\}_{i=1}^{2^{p-1}}$ the subset of the alphabet that consists of the points which lie in the right sub-plane of the constellation, one can write $\mathcal{C}=\tilde{\mathcal{C}}\cup(-\tilde{\mathcal{C}})$. Therefore, replacing the probabilities $P[x_k=\pm\tilde{c}_m]$ by their expressions in (16), injecting these APPs in (30) and using the identity $e^x+e^{-x}=2\cosh(x)$, it can be shown that:

$$\begin{aligned} D_\delta(k) = 2\beta_k\sum_{\tilde{c}_m\in\tilde{\mathcal{C}}}\exp\left\{-\frac{S^2|\tilde{c}_m|^2}{2\sigma^2}\right\}\mu_k(\tilde{c}_m) \\ \times\cosh\left(\frac{\Re\left\{\tilde{c}_m\ y_k^* S e^{j\phi}\right\}}{\sigma^2}+\frac{L_p(k)}{2}\right). \end{aligned} \tag{31}$$

It can also be shown that $\mu_k(\tilde{c}_m)$ can expressed as a recursive function of i as follows:

$$\mu_k(\tilde{c}_m) = \theta_{k,p}(i). \tag{32}$$

The initialization for $p=1$ (i.e., the basic BPSK constellation) is given by $\theta_{k,1}(.)=1$, since $\mu_k(\tilde{c}_m)=1\ \forall\ \tilde{c}_m\in\tilde{\mathcal{C}}_1$. Now, the term $D_\delta(k)$ can be ultimately written as follows:

$$D_\delta(k) = 2\beta_k\ F_p(u_k), \tag{33}$$

where $F_p(.)$ is given by:

$$\begin{aligned} F_p(x) = \sum_{i=1}^{2^{p-1}}\theta_{k,p}(i)\exp\left\{-\frac{S^2(2i-1)^2d_p^2}{2\sigma^2}\right\} \\ \times\cosh\left(\frac{(2i-1)d_pSx}{\sigma^2}+\frac{L_p(k)}{2}\right). \end{aligned} \tag{34}$$

where u_k defined as $u_k\triangleq\Re\left\{y_k^*e^{j(\phi+2\pi k\nu)}\right\}$ can be expressed as:

$$u_k = I_k\cos(2\pi k\nu+\phi)+Q_k\sin(2\pi k\nu+\phi). \tag{35}$$

Finally, the LF of y_k is given by:

$$p[y_k;\boldsymbol{\delta}] = \frac{1}{2\pi\sigma^2}\exp\left\{-\frac{I_k^2+Q_k^2}{2\sigma^2}\right\}2\beta_k\ F_p(u_k). \tag{36}$$

If we also define $v_k\triangleq\Im\left\{y_k^*e^{j(\phi+2\pi k\nu)}\right\}$, which can be developed into:

$$v_k = I_k\sin(2\pi k\nu+\phi)-Q_k\cos(2\pi k\nu+\phi), \tag{37}$$

using the fact that $I_k^2+Q_k^2 = u_k^2+v_k^2$, it can be shown that $p[y_k;\boldsymbol{\delta}]$ itself is factorized as follows:

$$p[y_k;\boldsymbol{\delta}] \quad = \quad p[u_k;\boldsymbol{\delta}]p[v_k;\boldsymbol{\delta}], \tag{38}$$

where the pdfs of u_k and v_k are given by:

$$p\big[u_k;\boldsymbol{\delta}\big] \;=\; \frac{2\beta_k}{\sqrt{2\pi\sigma^2}}\exp\left\{-\frac{u_k^2}{2\sigma^2}\right\}F_{p,\boldsymbol{\delta}}(u_k), \tag{39}$$

$$p\big[v_k;\boldsymbol{\delta}\big] \;=\; \frac{1}{\sqrt{2\pi\sigma^2}}\exp\left\{-\frac{v_k^2}{2\sigma^2}\right\}, \tag{40}$$

with

$$\beta_k = \frac{1}{2^p}\prod_{l=1}^{p}\frac{1}{\cosh\big(L_l(k)/2\big)}. \tag{41}$$

Moreover, we have $p[y_k^* e^{j(2\pi k\nu+\phi)};\boldsymbol{\delta}] = p[u_k,v_k;\boldsymbol{\delta}]$ since u_k and v_k are indeed the real and imaginary parts of $y_k^* e^{j(2\pi k\nu+\phi)}$. Furthermore, since the synchronization parameters ϕ and ν are assumed to be deterministic, we readily have $p[y_k^* e^{j(2\pi k\nu+\phi)};\boldsymbol{\delta}] = p[y_k^*;\boldsymbol{\delta}] = p[y_k;\boldsymbol{\delta}]$. This leads to $p[u_k,v_k;\boldsymbol{\delta}] = p[y_k;\boldsymbol{\delta}]$ which is combined with (38) to yield:

$$p[u_k,v_k;\boldsymbol{\delta}] \quad = \quad p[u_k;\boldsymbol{\delta}]p[v_k;\boldsymbol{\delta}], \tag{42}$$

meaning that u_k and v_k are indeed two independent random variables (RVs) which are distributed according to (39) and (40).

B. LLF for RQAM signals:

In the following, we will factorize the pdf $p[y_k;\boldsymbol{\delta}]$ in the R-QAM case. Furthermore, since the synchronization parameters ϕ and ν are assumed to be deterministic, we readily have $p[y_k;\boldsymbol{\delta}] = p[y_k^*;\boldsymbol{\delta}] = p[y_k^* e^{j(2\pi k\nu+\phi)};\boldsymbol{\delta}]$. On the other hand, since:

$$y_k = S\; x_k e^{j(2\pi k\nu+\phi)} + w_k, \tag{43}$$

we can establish that:

$$y_k^* e^{j(2\pi k\nu+\phi)} = S\; x_k^* + \tilde{w}_k, \tag{44}$$

where $\tilde{w}_k \triangleq w_k^* e^{j(2\pi k\nu+\phi)}$. We can now underline the following properties:

- Since w_k is a *circular* additive white gaussian noise (CAWGN), $\tilde{w}_k$ is a complex CAWGN with *independent* real and imaginary parts.
- Since the coded bits are assumed to be independent, the real and imaginary parts of x_k are independent. Consequently, the real and imaginary parts of $S\; x_k^*$ are independent.
- The noise samples w_k and the transmitted symbols x_k are independent. Hence, so are $\tilde{w}_k$ and $S\; x_k^*$.

Owing to these properties, we can deduce that $\Re\big\{y_k^* e^{j(2\pi k\nu+\phi)}\big\}$ and $\Im\big\{y_k^* e^{j(2\pi k\nu+\phi)}\big\}$ are independent. And these quantities are nothing but u_k and v_k defined in the previous subsection. Hence, we have:

$$p[y_k;\boldsymbol{\delta}] = p[u_k;\boldsymbol{\delta}]p[v_k;\boldsymbol{\delta}], \tag{45}$$

where, in this case, u_k and v_k, now have the following distributions:

$$p\big[u_k;\boldsymbol{\delta}\big] \;=\; \frac{2\beta_{k,1}}{\sqrt{2\pi\sigma^2}}\exp\left\{-\frac{u_k^2}{2\sigma^2}\right\}F_{p_1,\boldsymbol{\delta}}(u_k), \tag{46}$$

$$p\big[v_k;\boldsymbol{\delta}\big] \;=\; \frac{2\beta_{k,2}}{\sqrt{2\pi\sigma^2}}\exp\left\{-\frac{v_k^2}{2\sigma^2}\right\}F_{p_2,\boldsymbol{\delta}}(v_k), \tag{47}$$

with

$$\beta_{k,1} = \frac{1}{2^{p_1}}\prod_{l=1}^{p_1}\frac{1}{\cosh\big(\frac{L_l(k)}{2}\big)}, \tag{48}$$

$$\beta_{k,2} = \frac{1}{2^{p_2}}\prod_{l=p_1+1}^{p_1+p_2}\frac{1}{\cosh\big(\frac{L_l(k)}{2}\big)}, \tag{49}$$

where, in (46) and (47), we resort to the same function $F_{p,\boldsymbol{\delta}}(x)$ used in the case of PAM constellations, yet with sums over p_1 terms for u_k and p_2 terms for v_k in the RQAM case. Also the additive term inside the cosh changes from $\frac{L_p(k)}{2}$ in the PAM case to $\frac{L_{p_1}(k)}{2}$ (last bit of the first group of bits) and $\frac{-L_{p_1+p_2}(k)}{2}$ (last bit of the second group of bits) for u_k and v_k, respectively, in the RQAM case[5].

The above factorization of $p[y_k;\boldsymbol{\delta}]$ is actually the cornerstone result behind enabling for the very first time the derivation in the next section of the analytical expressions for the considered stochastic CRLBs over RQAM[6] transmissions.

V. Derivation of the CA CRLBs

Our starting point is the expression of the FIM elements defined in (5). And we are now ready to find the explicit expression for the global LLF, $L(\boldsymbol{y};\delta) \triangleq \ln(p[\boldsymbol{y};\boldsymbol{\delta}])$. In fact, by injecting (36) in (27), it follows that:

$$L(\boldsymbol{y};\boldsymbol{\delta}) = -K\ln\big(2\pi\sigma^2\big) + \sum_{k=k_0}^{k_0+K-1}\ln\big(D_{\boldsymbol{\delta}}(k)\big) - \frac{I_k^2+Q_k^2}{2\sigma^2}. \tag{50}$$

A. Derivation of $\boldsymbol{I}(\boldsymbol{\delta})$:

1) PAM constellations: For PAM constellations, after recalling that $D_{\boldsymbol{\delta}}(k) = 2\beta_k F_{p,\boldsymbol{\delta}}(u_k)$ and dropping all the terms which are irrelevant when deriving with respect to the couple ϕ, the LLF defined above becomes:

$$L(\boldsymbol{y};\boldsymbol{\delta}) = \sum_{k=k_0}^{k_0+K-1}\ln\big(F_{p,\boldsymbol{\delta}}(u_k)\big). \tag{51}$$

The FIM term pertaining to the phase ϕ is then given by:

$$\mathrm{E}_{\boldsymbol{y}}\left\{\frac{\partial^2\ln(p[\boldsymbol{y};\boldsymbol{\delta}])}{\partial\phi^2}\right\} = \sum_{k=k_0}^{k_0+K-1}\mathrm{E}\left\{\frac{\partial^2\ln(F_p(u_k))}{\partial\phi^2}\right\}. \tag{52}$$

The first diagonal term of $\boldsymbol{I}(\boldsymbol{\delta})$, denoted as $\eta_{k,p} \triangleq \mathrm{E}\big\{\partial^2\ln\big(F_p\big(u_k\big)\big)/\partial\phi^2\big\}$, is obtained in this case as follows:

$$\eta_{k,p}(\rho) = -4\rho\Phi_{k,p}(\rho), \tag{53}$$

where $\Phi_{k,p}(.)$ is given by:

$$\Phi_{k,p}(\rho) = \frac{d_p^2\beta_{k,p}}{\sqrt{2\pi}}\int_{-\infty}^{+\infty}\frac{\chi_{k,p}^2(t,\rho)}{\delta_{k,p}(t,\rho)}\;\; e^{-\frac{t^2}{2}}\,dt, \tag{54}$$

[5]The minus one "-1" in the $\frac{-L_{p_1+p_2}(k)}{2}$ is due to the minus one "-1" in $v_k = -S\;\Im\{x_k\} + \Im\{\tilde{w}_k\}$.

[6]Decomposing it into two terms analogous to the PAM term in the PAM LF, which will turn out to be simple to handle in the FIM elements calculations.

where, by using $\omega_{k,p}^{(l)}(i) \triangleq (2i-1)^l \theta_{k,p}(i)\ e^{-(2i-1)^2 d_p^2 \rho}$, the functions $\delta_{k,p}(.,.)$ and $\chi_{k,p}(t,\rho)(.,.)$ are given by:

$$\delta_{k,p}(\rho,t) = \sum_{i=1}^{2^{p-1}} \omega_{k,p}^{(0)}(i)\cosh(t_{i,p}), \quad (55)$$

$$\chi_{k,p}(t,\rho) = \sum_{i=1}^{2^{p-1}} \omega_{k,p}^{(1)}(i)\sinh(t_{i,p}). \quad (56)$$

where $t_{i,p} = \sqrt{2\rho}(2i-1)d_p t + \frac{L_p(k)}{2}$.

2) RQAM constellations: The first diagonal term of $\boldsymbol{I}(\boldsymbol{\delta})$ is composed of two terms. The first one, defined as $\gamma_{k,p_1} \triangleq \mathrm{E}\left\{\partial^2 \ln\left(F_{p_1}(u_k)\right)/\partial\phi^2\right\}$, can be obtained after some algebraic manipulations as:

$$\gamma_{k,p_1}(\rho) = 4c_{2,p_2}^{(k)}\rho\left[c_{2,p_1}^{(k)}\rho - 2\Phi_{k,p_1}(\rho)\left(\frac{1}{2c_{2,p_2}^{(k)}} + \rho\right)\right]. \quad (57)$$

where

$$c_{1,p_j}^{(k)} = S2\beta_{k,p_j} d_{p_1+p_2} \sinh\left(\frac{-L_{p_j}(k)}{2}\right)\sum_{i=1}^{2^{p_j-1}} \theta_{k,p_j}(i)(2i-1). \quad (58)$$

The second term, $\gamma_{k,p_2} \triangleq \mathrm{E}\left\{\partial^2 \ln\left(F_{p_2}(v_k)\right)/\partial\phi^2\right\}$, can be easily deduced from the expression of $\gamma_{k,p_1}(\rho)$ in (57). This is due to the apparent symmetries in the pdfs of the two RVs u_k and v_k, as seen from (46) and (47), leading to:

$$\gamma_{k,p_2}(\rho) = 4c_{2,p_1}^{(k)}\rho\left[c_{2,p_2}^{(k)}\rho - 2\Phi_{k,p_2}(\rho)\left(\frac{1}{2c_{2,p_1}^{(k)}} + \rho\right)\right], \quad (59)$$

where in this case, we use $d_{p_1+p_2}$ instead of d_p in both $\Phi_{k,p_1}(\rho)$ and $\Phi_{k,p_2}(\rho)$. Lastly, the first diagonal element of the FIM follows immediately as:

$$-\mathrm{E}\left\{\frac{\partial^2 \ln\left(p[\boldsymbol{y};\boldsymbol{\delta}]\right)}{\partial\phi^2}\right\} = -\sum_{k=k_0}^{k_0+K-1}\left[\ \gamma_{k,p_1}(\rho) + \gamma_{k,p_2}(\rho)\ \right]. \quad (60)$$

Deriving the other elements using equivalent manipulations and defining $\Omega_k(\rho) \triangleq -\gamma_{k,p_1}(\rho) - \gamma_{k,p_2}(\rho)$ for RQAM and $\Omega_k(\rho) \triangleq -\eta_{k,p}(\rho)$ for PAM, we obtain an analytical expression for the FIM as follows:

$$\boldsymbol{I}(\boldsymbol{\delta}) = \sum_{k=k_0}^{k_0+K-1}\Omega_k(\rho)\begin{pmatrix} 1 & 2\pi k \\ 2\pi k & (2\pi k)^2 \end{pmatrix} = \sum_{k=k_0}^{k_0+K-1}\boldsymbol{I}_k(\boldsymbol{\delta}), \quad (61)$$

where $\boldsymbol{I}_k(\boldsymbol{\delta})$ is the FIM pertaining to the k^{th} received sample. We underline here the fact that the FIM associated with the synchronization parameters depends on the first time index k_0 as seen from (61). Such dependency on the observation window has been previously reported in the literature even in the NDA case. Likewise, we obtain in CA estimation different bounds as k_0 varies. Our interest is focused on the best bound which is obtained when the square of the off-diagonal elements is negligible compared to the product of the diagonal ones, i.e., when ϕ and ν are *decoupled*. We verify by simulations that ϕ and ν turn out to be *decoupled* when the set of sampling indices is centred around zero, i.e., $k_0 = -\frac{K-1}{2}$. In this case, the CRLBs' expressions reduce to:

$$\mathrm{CRLB}_{\mathrm{CA}}(\nu) = \frac{1}{(2\pi)^2}\left(\sum_{k=-\frac{K-1}{2}}^{\frac{K-1}{2}}\ \Omega_k(\rho)k^2\right)^{-1}, \quad (62)$$

$$\mathrm{CRLB}_{\mathrm{CA}}(\phi) = \left(\sum_{k=\frac{K-1}{2}}^{\frac{K-1}{2}}\ \Omega_k(\rho)\right)^{-1}. \quad (63)$$

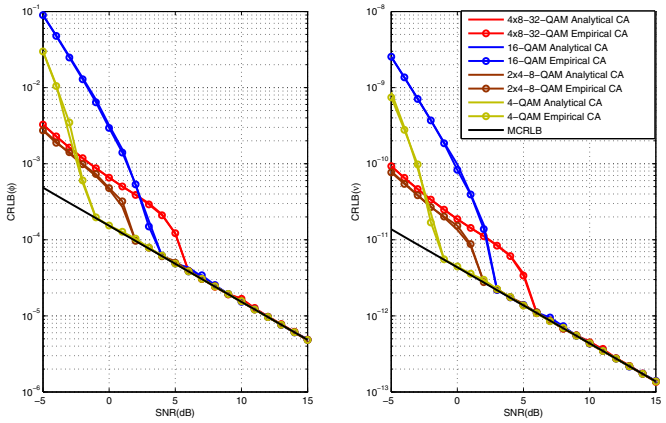

Fig. 1. Analytical and empirical CA CRLBs of: a) the phase, and b) the CFO, for different RQAM modulations and coding rate $R_c = 1/3$.

We notice that the FIM of (ϕ,ν) is independent of ϕ and ν, which means that the best achievable accuracy (i.e., CRLB) is of the same level regardless of the values taken by ϕ or ν.

VI. Simulation Results

In this section, we illustrate by simulations the new closed-form CRLBs of the different parameters with various modulation orders and different coding rates using $K = 3270$ coded symbols each time. The turbo code consists of two identical RSCs both of nominal rate $R_0 = 1/2$ and of generator polynomials (1,1,0,1) and (1,0,1,1), respectively. The puncturer is configured so as to obtain the desired overall coding rate R_c. For the tailing bits, the size of the RSC encoders memory is fixed to 4.

In order to evaluate the obtained CA estimation CRLBs, the extrinsic information delivered by the SISO decoder is used to evaluate the bit LLRs, $L_l(k)$. Once having the LLRs at hand, it is possible to evaluate all the quantities involved in the expressions of the new bounds. In all simulations, we use the *extrinsic* information obtained at the 8^{th} turbo iteration. In fact, the latter are iteratively exchanged between the two SISO decoders until achieving steady state after which the aforementioned soft values remain almost unchanged.

We start by verifying in Fig. 1 that the newly obtained closed-form expressions for the CA CRLBs coincide with their *empirical* counterparts obtained previously in [9, 10] for both ϕ and ν. Indeed, an extremely large number of noisy observations was generated in order to find an empirical value for the expectation involved in the FIM for the considered parameters. In contrast, our new closed-form expressions allow the immediate evaluation of the CRLBs from any turbo-coded PAM and RQAM signals. Furthermore, we observe that there is no *strict order* relationship holding over the entire SNR range between the CRLBs and the modulation size (i.e., the former increasing with the latter) in the most general case of RQAM modulations mixing both square and non-square QAM. However, within each of these two sub-classes, such order relationship holds indeed (i.e., 8-QAM<32-QAM and 4-QAM<16-QAM).

We plot in Fig. 2 the CA CRLBs for different PAM modulation orders. As expected, we verify that the CA CRLBs are smaller than the NDA CRLBs derived recently in [8]. This predicted result highlights and quantifies the potential estimation performance gain that could be achieved by leveraging the information about the

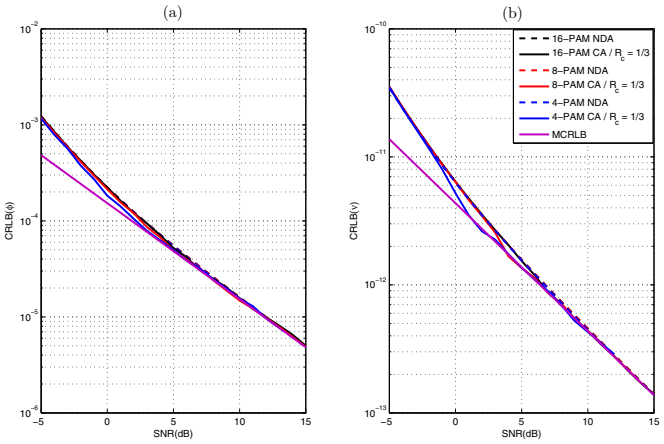

Fig. 2. Analytical CA and NDA CRLBs of: a) the phase, and b) the CFO, for different PAM modulations and $R_c = 1/3$.

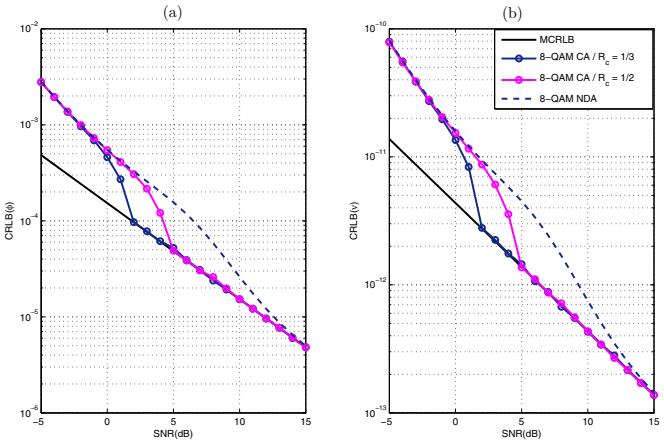

Fig. 3. Analytical CA CRLBs of : a) the phase, and b) the CFO, and for different coding rates and 2x4-8-QAM modulation.

transmitted bits one could gather during the decoding process. It is in contrast with the traditional NDA scheme where the considered parameters are estimated directly from the output of the matched filter. Additionally and most prominently, the CA CRLBs decrease rapidly and reach the DA CRLBs, the ideal bounds that would be obtained if all the transmitted symbols were perfectly known to the receiver, which are given by:

$$\text{MCRLB} = \begin{cases} \dfrac{1}{2K\rho} & \text{for the phase,} \\ \dfrac{6}{(2\pi)^2 K(K^2-1)\rho} & \text{for the CFO.} \end{cases} \tag{64}$$

We also notice that the CA CRLB for the 4-PAM modulation is distinctly lower than the CA CRLB for higher orders. In fact, when the order is greater than 4, all CA CRLBs start to approach each other very fast to the point where we can hardly notice any visible improvement from using higher-order PAM. Similar performance behavior has been previously reported [8,13] in the case of NDA estimation.

In Fig. 3, we illustrate the effect of the coding rate on the turbo estimation performance by plotting the CRLBs with 2x4-8-QAM modulation and the two coding rates $R_c = 0.3285 \approx \frac{1}{3}$ and $R_c = 0.4892 \approx \frac{1}{2}$. Even though the CA CRLBs corresponding to the two considered rates ultimately coincide at moderate SNR levels, they exhibit a significant gap at lower SNR values. In fact, with smaller coding rates, more redundancy can potentially be provided by the turbo encoder and the bits could then be decoded more accurately. In this case, the *extrinsic* information, which is used to approximate the LLRs, becomes increasingly higher (in absolute value) and CA estimation becomes even closer in CRLB performance to DA estimation.

VII. Conclusion

In this paper, we established for the first time analytical expressions of the CRLBs for joint channel phase and CFO estimation from turbo-coded PAM- and RQAM-modulated signals over *flat-fading* channels. The properties of Gray-labeled PAM and RQAM constellations enabled us to simplify the LLF and calculate the FIM elements and, hence, the considered CRLBs in closed-form. The obtained bounds coincide with the empirical ones already reported in the literature and range between the NDA and DA CRLBs, thereby highlighting and quantifying the advantage of CA over NDA or DA estimation. At high SNR, the CA CRLBs coincide with the DA bounds thereby implying near-optimal CA estimation performance in that regime. With PAM signals, the CRLBs saturate when the modulation order increases, meaning that no further losses in estimation accuracy occur from use of higher-order PAMs. Besides, within square-QAM or non-square-QAM RQAM signals, we verify that the CRLBs increase with either the modulation order or the coding rate.

References

[1] C. Berrou, "The ten-year old turbo codes are entering into service", *IEEE J. Commun. Mag.*, vol. 41, no. 8, pp. 110-116, Aug. 2003.

[2] 3GPP TS 36.211: 3rd Generation Partnership Project, *Technical Specification Group Radio Access Network; Evolved Universal Terrestrial Radio Access (E-UTRA); Physical Channels and Modulation*.

[3] W. Gappmair, R. Lopez-Valcarce, and C. Mosquera, "Joint NDA estimation of carrier frequency/phase and SNR for linearly modulated signal", *IEEE Signal Process. Lett.*, vol. 17, no. 5, pp. 517-520, May 2010.

[4] K. Choi, "Residual frequency offset compensation-embedded turbo decoder," *IEEE Trans. Vehic. Technol.*, vol. 57, no. 5, pp. 3211-3217, May 2008.

[5] S. M. Kay, *Fundamentals of Statistical Signal Processing, Vol. 1: Estimation Theory*, Englewood Cliffs, NJ: Prentice-Hall, 1998.

[6] J. P. Delmas "Closed form-expressions of the exact Cramér-Rao bound for parameter estimation of BPSK, MSK, or QPSK waveforms," *IEEE Signal Process. Lett.*, vol. 15, pp. 405-408, 2008.

[7] F. Bellili, N. Atitallah, S. Affes, and A. Stéphenne, "Cramér-Rao lower bounds for frequency and phase NDA estimation from arbitrary square QAM-modulated signals," *IEEE Trans. Signal Process.*, vol. 58, no. 9, pp. 4517-4525, Sep. 2010.

[8] A. R.-Kebrya, I.-M. Kim, D. I. Kim, F. Chan, and R. Inkol , "Likelihood-based modulation classification for multiple-antenna receiver", *IEEE Trans. Commun.*, vol. 61, no. 9, pp. 3816-3829, Sep. 2013.

[9] N. Noels, H. Steendam, and M. Moeneclaey, "Carrier and clock recovery in (turbo) coded systems: Cramér-Rao bound and synchronizer performance," *EURASIP J. App. Signal Process., Special Issue on Turbo Processing,* vol. 2005, no. 6, pp. 972-980, May 2005.

[10] N. Noels, H. Steendam, and M. Moeneclaey, "The Cramér-Rao bound for phase estimation from coded linearly modulated signals," *IEEE Commun. Lett.*, vol. 7, no. 5, pp. 207-209, May 2003.

[11] U. Mengali and A. N. D'andrea, *Synchronization Techniques for Digital Receivers,* New York: Plenum, 1997.

[12] F. Bellili, A. Methenni, and S. Affes, "Closed-form CRLBs for CFO and phase estimation from turbo-coded square-QAM-modulated transmissions," *IEEE Trans. Wireless Commun.*, vol. 14, no. 5, pp. 2513-253, May 2015.

[13] N. Noels, *Synchronization in Digital Communication S ystems: Performance Bounds and Practical Algorithms,* Ph.D. Dissertation, Ghent University, Belgium, 2009.